JOURNAL OF MATERIALS SCIENCE 24 (1989) 2433–2436

Strengthening in the Cu–9Ni–1.2Sn alloy

P. KRATOCHVÍL, J. PEŠIČKA
Faculty of Mathematics and Physics, Charles University, Department of Metal Physics, Ke Karlovu 5, Prague 2, Czechoslovakia

Data are presented describing quantitatively the structure development in the Cu–9.7 at % Ni–1.2 at % Sn alloy during ageing at 673 K. On the basis of these results the contributions to the strength of the alloy from different structure types are evaluated. These are discussed with respect to their additivity.

1. Introduction

The properties of the Cu–Ni–Sn alloys have been examined [1–7] over many years, especially from the point of view of those with spinodal composition. The tin content and temperature of annealing determine the sequence of structures originating during decomposition. At 673 K the Cu–9.7 at % Ni–3.0 at % Sn and Cu–9.7 at % Ni–2.7 at % Sn alloys decompose by spinodal decomposition followed by nucleation and growth of $(Cu_xN_{1-x})_3$ Sn particles (with DO_{22} structure changing into DO_3 structure after very long ageing). On the other hand, the Cu–9.7 at % Ni–1.2 at %Sn alloy decomposes after an incubation period by nucleation and growth of $(Cu_xN_{1-x})_3$ Sn particles (here also DO_{22} structure transforms finally into DO_3 structure). The structure has been always investigated by transmission electron microscopy (TEM) and electron diffraction (ED) [1–7].

There is a lack of quantitative experimental data describing the microstructure. This problem is solved in this paper with respect to the data needed for evaluating the strengthening contributions in the Cu–9.7 at % Ni–1.2 at % Sn alloy.

2. Experimental results

Specimens were prepared from 0.3 mm sheets of the Cu–9.7 at % Ni–1.2 at % Sn alloy. These were aged for 2 h at 1073 K (solution treatment), water quenched and then they were aged at 673 K for various time intervals in argon. The resulting grain size after solution treatment was 50 to 60 μm and it remained constant during ageing at 673 K [3]. Thereafter the specimens were deformed in tension at 4 K. The initial strain rate was 4×10^{-4} sec^{-1}.

The microstructure of the specimen was investigated by TEM and ED for seven different ageing times. Coherent metastable particles of DO_{22} structure were observed. In order to gather enough details on the structure, the following images were taken from each area of interest: (a) a pair of stereomicrographs, (b) bright-field image, (c) dark-field image micrographs. The size of the particles was determined from the dark-field images using the superstructure spots. The particles are cylinders of diameter $2r_0$ and length, d (see Table I). The number of particles, N, was determined in the indentical volume, V, of each specimen (3.645×10^7 nm^3). The thickness of the specimen was determined using stereomicrographs by a method which was described elsewhere [8]. The error in the specimen thicknesses determination is 10% or less. The misfit

$$\varepsilon = \frac{a_p - a_M}{a_M}$$

where a_p is the lattice parameter of the particles and a_M is the lattice parameter of the matrix, was determined by comparing the sizes in the bright and dark-field images. The misfit was determined to be $\varepsilon = (1.0 \pm 0.3) \times 10^{-2}$ and to be independent of ageing time. The structural data are summarized in Table I. On the basis of these data other structural parameters can be calculated, such as the particle volume, V_p, the fraction volume, f, and concentration of the tin atoms in the matrix. They are summarized in Table II.

TABLE I

t (sec)	r_0 (nm)	d (nm)	N
0	–	–	–
10^4	2.0 ± 1.0	sphere	4 ± 1
3.5×10^4	2.0 ± 0.7	sphere	140 ± 10
10^5	2.5 ± 0.7	13.5 ± 2.0	198 ± 20
3.5×10^5	2.9 ± 0.7	16.0 ± 2.0	350 ± 30
8×10^5	5.5 ± 1.0	36.0 ± 2.0	207 ± 20
10^6	5.7 ± 1.0	38.0 ± 2.0	214 ± 20

The nickel atoms dissolve well in the copper matrix without any restriction and it is supposed that the concentration of the nickel atoms, C_{Ni}, is constant during the ageing process, $C_{Ni} = 9.7$ at %. The concentration of tin at the stable solvus line, C_{ss}, is

TABLE II

t (sec)	V_p (nm^3)	C_{sn} (at %)	f
0	0	1.20	0
10^4	33.5	1.20	$(3.6 \pm 3.6) \times 10^{-6}$
3.5×10^4	33.5	1.19	$(1.3 \pm 0.9) \times 10^{-4}$
10^5	265	1.16	$(1.4 \pm 0.8) \times 10^{-3}$
3.5×10^5	423	1.10	$(4.1 \pm 2.0) \times 10^{-3}$
8×10^5	3420	0.73	$(2.0 \pm 0.7) \times 10^{-2}$
10^6	3880	0.66	$(2.3 \pm 0.8) \times 10^{-2}$

0022–2461/89 $03.00 + .12

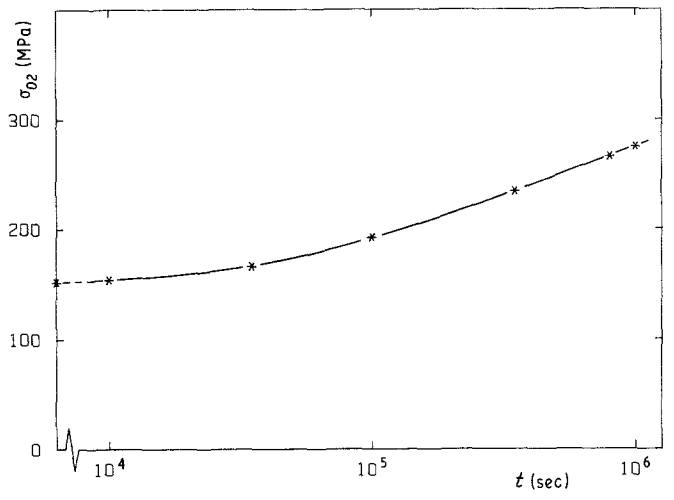

Figure 1 The dependence of the yield stress on the ageing time.

0.80 at % at 673 K [9]. The change in tin concentration during ageing (see Table II) suggests that the concentration of tin at metastable solvus line, C_{ms}, is 0.66 at % or lower at 673 K. Assuming $C_{ms} = 0.6$ at %, the maximal volume fraction of metastable particles, $f_{max} = 2.3 \times 10^{-2}$. The data from Tables I and II are plotted in Figs 2 and 3.

In our recent paper, the incubation period is estimated as $\sim 10^5$ sec [3]. More precise investigation of the structure development shows that the incubation period is 10^4 sec. It is obvious from Fig. 2 that after the incubation period (10^4 sec) first the nucleation of the particles takes place (the number of particles increases, while their volume remains constant). For an ageing time of 3.5×10^5 sec the number of particles reaches a maximum. For longer times the number of particles decreases and the volume of the particles quickly grows. This means that ripening of the particles occurs. The slope of the dependence $\log \{-\ln [1 - (f/f_{max})]\}$ on $\log t$ (Fig. 3) is the kinetic coefficient, n, of the decomposition reaction. From the Avrami plot (Fig. 3), $n = 1.7$ follows. This value corresponds to the decomposition reaction where first volume nucleation takes place and then ripening occurs [10].

3. Discussion

During the ageing process the $(Cu_xNi_{1-x})_3Sn$ particles appear in the specimens and they contribute to the strengthening of the specimens together with the solid solution hardening. The structural parameters (Tables I and II) enable evaluation of both contributions to be made. The strength increase, $\Delta\sigma_{02}^{SS}$, by solid solution is given [11] by

$$\Delta\sigma_{02}^{SS} = m \frac{\mu}{Z} \varepsilon_e^{4/3} C^{2/3} \quad (1)$$

where $m = 3.1$ (Taylor factor), μ is the shear modulus, $\mu = 4.21 \times 10^4$ MPa, $Z = 750$ is a numerical constant, C is the concentration and ε_e is the interaction parameter. According to [12]

$$\varepsilon_e = (\eta^2 + \alpha^2\delta^2)^{1/2} \quad (2)$$

where $\alpha = 19$, $\eta = (\partial\mu/\partial C)/(1/C)$ is the shear modulus misfit and $\delta = (\partial b/\partial C)/(1/\mathbf{b})$ is size misfit, $\mathbf{b}$ is the magnitude of Burgers vector. For solid solution of nickel in copper, $\varepsilon_e = 0.87$ [12] and for solid solution of tin in copper, $\varepsilon_e = 6.08$ [13]. Then $\Delta\sigma_{02}^{Ni} = 30$ MPa independent of ageing time, while $\Delta\sigma_{02}^{Sn}$ depends on ageing time because of the changing tin content in the matrix (see Table III). The coherent particles have a cylindrical shape and they are oriented along the $\langle 1\,0\,0 \rangle$ directions. Saxlová and Balík [14] estimated hardening increase caused by such particles

$$\Delta\sigma_{02}^{P} = 3.1 \times 143 f^{1/2} \lambda^{1/2} \alpha^{-1/2} \quad (3)$$

where λ is the distance of the particle centres ($\lambda = (V/N)^{1/3}$) and $\alpha = d/2r_0$. The values $\Delta\sigma_{02}^{P}$ calculated with the help of Equation 3 are given in Table III. The single contributions to the strengthening $\Delta\sigma_{02}^{Ni}$, $\Delta\sigma_{02}^{Sn}$ and $\Delta\sigma_{02}^{P}$, together with the $\sigma_{02}^{Cu} = 37$ MPa [15]

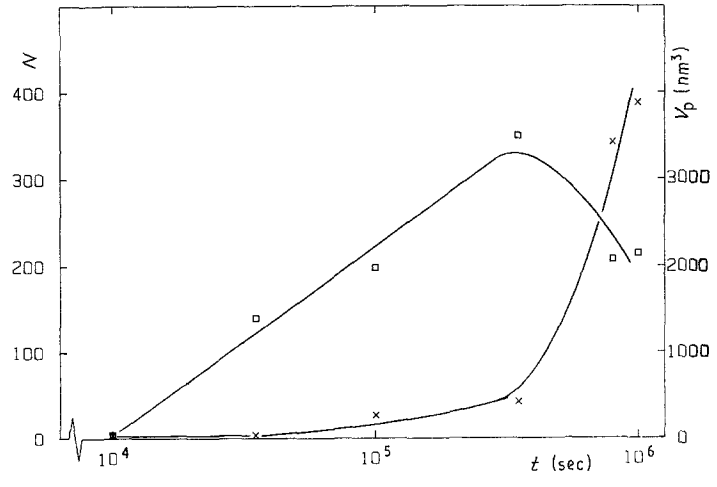

Figure 2 The dependence of (×) the particle volume and (□) the number of particles on ageing time.

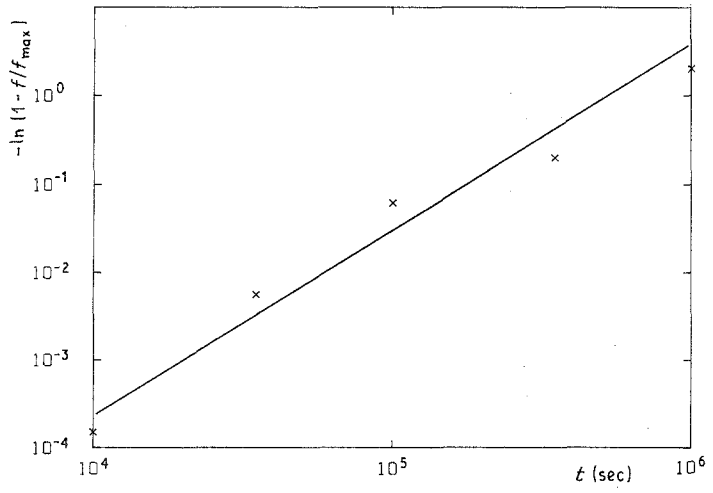

Figure 3 The dependence of log $[-\ln(1 - f/f_{max})]$ on log t.

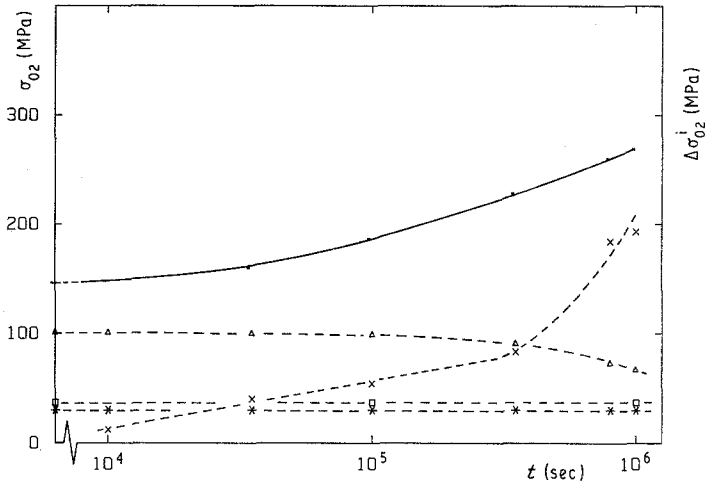

Figure 4 The dependences of (——) yield stress σ_{02}^{exp}, (□) σ_{02}^{Cu}, yield stress increases (*) $\Delta\sigma_{02}^{Ni}$ (△), $\Delta\sigma_{02}^{Sn}$ and (x) $\Delta\sigma_{02}^{P}$, on ageing time.

(σ_{02}^{Cu} is the yield stress of pure polycrystal copper at 4.2 K) are plotted in Fig. 4.

The question should be solved how to obtain total strengthening from single contributions. On the basis of computer simulations, Foreman and Makin [16] suggested a solution of this problem for several combinations of obstacle strength. In the case of two kinds of weak obstacles, their results prefer the quadratic addition, while for the case of several hard obstacles among many weak obstacles, the linear addition holds. The microstructure of the Cu–9.7 at % Ni–1.2 at % Sn alloy corresponds to the combination of two kinds of weak obstacles – nickel atoms and tin atoms – and one kind of hard obstacle – the coherent particles. In agreement with Foreman and Makin [16] the quadratic addition was applied for the addition of both solution strengthening increases $\Delta\sigma_{02}^{Ni}$ and $\Delta\sigma_{02}^{Sn}$. Then the linear addition was used to combine the total solid solution strengthening with coherent particle hardening. The results are given in Table IV, in which σ_{02}^{exp} is the experimental value of the yield stress. Agreement is seen between the second column in Table IV (the experimental values) and the third one (the evaluation of strengthening on the basis of the determined structural quantities).

Very recently Büttner *et al.* [17] again tried [18, 19] to describe the addition of the solid solution hardening with the coherent particle hardening in a ternary CuAu–Co system. We were not able to describe our experimental data in the way they did. No unique value of k exists in the equation

$$(\sigma_{02}^{exp} - \sigma_{02}^{Cu})^k = (\Delta\sigma_{02}^{Ni})^k + (\Delta\sigma_{02}^{Sn})^k + (\Delta\sigma_{02}^{P})^k \quad (4)$$

describing the mutual influence of both types of obstacles for our whole series of samples, i.e. depending on the annealing treatment.

We understand that more experimental data must be gathered before the final solution of the problem (hardening contributions and their additivity) is found.

TABLE III

t (sec)	$\Delta\sigma_{02}^{Ni}$ (MPa)	$\Delta\sigma_{02}^{Sn}$ (MPa)	$\Delta\sigma_{02}^{P}$ (MPa)
0	30	101	0
10^4	30	101	12
3.5×10^4	30	100	40
10^5	30	99	54
3.5×10^5	30	91	83
8×10^5	30	73	184
10^6	30	67	193

TABLE IV

t (sec)	$\sigma_{02}^{exp} - \sigma_{02}^{Cu}$ (MPa)	$(\Delta\sigma_{02}^{Sn2} + \Delta\sigma_{02}^{Ni2})^{1/2} + \Delta\sigma_{02}^{P}$ (MPa)
0	114	105
10^4	116	117
3.5×10^4	128	144
10^5	154	157
3.5×10^5	196	179
8×10^5	228	263
10^6	237	266

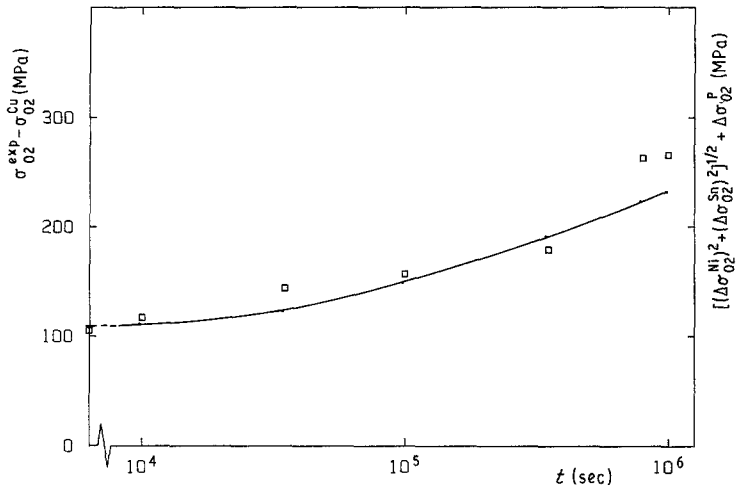

Figure 5 The comparison of the experimental value (——) $\sigma_{02}^{exp} - \sigma_{02}^{Cu}$ with (□) the results of addition.

4. Conclusions

1. The Cu–9.7 at % Ni–1.2 at % Sn alloy is hardened during annealing by $(Cu_xNi_{1-x})_3Sn$ particles of DO_{22} structure. These particles have a cylindrical shape. The size of the particles, the volume fraction and the misfit were found for seven different ageing times.

2. After the incubation period, the nucleation of the particles takes place followed by the ripening process.

3. On the basis of experimentally estimated structural parameters, the contributions of each type of obstacle were determined.

4. The contributions of solid solution strengthening increases are added quadratically. The total solid solution hardening is then added linearly with the particle hardening. Satisfactory agreement is obtained with experimental data.

References

1. M. KATO, S. KATSUTA and S. OKAMINE, *Mater. Sci. Engn* **77** (1986) 95.
2. L. H. SCHWARTZ and J. T. PLEWES, *Acta Metall.* **22** (1974) 911.
3. P. KRATOCHVÍL, J. MENCL, J. PEŠIČKA and S. N. KOMNIK, *Acta Metall.* **32** (1984) 1493.
4. V. I. DOTSENKO, P. KRATOCHVÍL, J. PEŠIČKA and P. WIELKE, *Czech. J. Phys. B* **31** (1981) 209.
5. M. KATO, T. MORI, L. H. SCHWARTZ, *Acta Metall.* **28** (1980) 285.
6. E. G. BARBURAJ, U. D. KULKARNI, E. S. K. MENON, R. KRISHAN, *J. Appl. Crystallogr.* **12** (1979) 476.
7. S. SHEKHAR, T. C. LEE, K. N. SUBRAMANIAN, *Phys. Status Solidi (a)* **91** (1985) 63.
8. A. DLOUHÝ and J. PEŠIČKA, *Czech. J. Phys.* (1989) to be published.
9. P. SAJDL, Diploma Thesis, Charles University, Prague (1985).
10. J. W. CHRISTIAN, "The theory of transformations in metals and alloys" (Pergamon, Oxford, 1975).
11. R. LABUSCH, *Acta Metall.* **20** (1972) 917.
12. B. SMOLA, *Czech. J. Phys. B* **31** (1981) 447.
13. R. L. FLEISCHER, *Acta Metall.* **11** (1963) 203.
14. M. SAXLOVÁ and J. BALÍK, *Czech. J. Phys. B* **31** (1981) 215.
15. LANDOLT-BÖRNSTEIN, "Zahlenwerte und Funktionen, 4 Band 2b Sinterwerkstoffe-Schweremetalle" (Springerverlag, Berlin, Heidelberg, 1964) p. 698.
16. A. J. E. FOREMAN and M. J. MAKIN, *Can. J. Phys.* **45** (1967) 511.
17. N. BÜTTNER, K.-D. FUSENIG and E. NEMBACH, *Acta Metall.* **35** (1987) 845.
18. E. NEMBACH, M. BÜTTNER and K.-D. FUSENIG, in Proceedings of the 7th International Conference on the Strength of Metals and Alloys, Montreal, edited by H. J. McQueen, J.-P. Bailon, J. I. Dickson, J. J. Jones and M. G. Akben (Pergamon, Oxford, 1985) p. 385.
19. M. BÜTTNER and E. NEMBACH, *Z. Metallkde.* **76** (1985) 82.

Received 29 March
and accepted 1 August 1988